Inference of selective force on house mouse genomes during secondary contact in East Asia

Kazumichi Fujiwara, Shunpei Kubo, Toshinori Endo, et al.

Genome Res. published online March 20, 2024
Access the most recent version at doi:10.1101/gr.278828.123

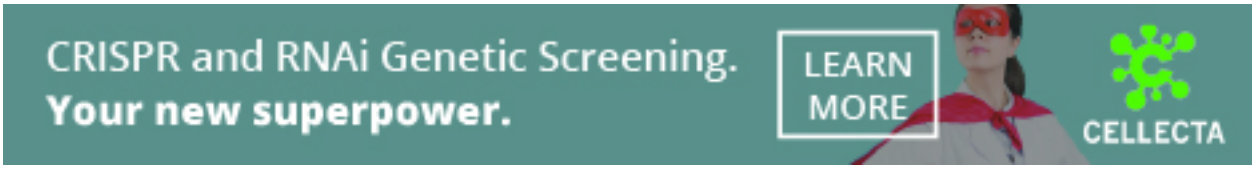

Inference of selective force on house mouse genomes during secondary contact in East Asia

Kazumichi Fujiwara[1,2], Shunpei Kubo[2], Toshinori Endo[2], Toyoyuki Takada[3], Toshihiko Shiroishi[4], Hitoshi Suzuki[5], Naoki Osada[2,*]

[1]Mouse Genomics Resource Laboratory, National Institute of Genetics, Mishima, Japan

[2]Graduate School of Information Science and Technology, Hokkaido University, Sapporo, Japan

[3]Integrated BioResource Information Division, RIKEN BioResource Research Center, Tsukuba, Japan

[4]RIKEN BioResource Research Center, Tsukuba, Japan

[5]Graduate School of Environmental Science, Hokkaido University, Sapporo, Japan

*Author for correspondence: Naoki Osada, Graduate School of Information Science and Technology, Hokkaido University, Sapporo, Japan; phone: +81-11-706-7332; email: nosada@ist.hokudai.ac.jp

Running title: East Asian wild house mouse genome analysis

Abstract

The house mouse (*Mus musculus*), which is commensal to humans, has spread globally via human activities, leading to secondary contact between genetically divergent subspecies. This pattern of genetic admixture can provide insights into the selective forces at play in this well-studied model organism. Our analysis of 163 house mouse genomes, with a particular focus on East Asia, revealed substantial admixture between the subspecies *castaneus* and *musculus*, particularly in Japan and southern China. We revealed, despite the different level of autosomal admixture among regions, that all Y Chromosomes in the East Asian samples belonged to the *musculus*-type haplogroup, potentially explained by genomic conflict under sex-ratio distortion due to varying copy numbers of ampliconic genes on sex chromosomes, *Slx* and *Sly*. Our computer simulations, designed to replicate the observed scenario, demonstrate that the preferential fixation of *musculus*-type Y Chromosomes can be achieved with a 10–20% increase in the male-to-female birth ratio. We also investigated the influence of selection on the post-hybridization of the subspecies *castaneus* and *musculus* in Japan. Even though the genetic background of most Japanese samples closely resembles the subspecies *musculus*, certain genomic regions overrepresented the *castaneus*-like genetic components, particularly in immune-related genes. Furthermore, a large genomic block (~2 Mbp) containing a vomeronasal/olfactory receptor gene cluster predominantly harbored *castaneus*-type haplotypes in the Japanese samples, highlighting the crucial role of olfaction-based recognition in shaping hybrid genomes.

Introduction

The house mouse (*Mus musculus*), an important laboratory animal, is commensal to humans and has spread worldwide due to human activities such as colonization, agricultural expansion, and trade (Gündüz et al. 2001; Geraldes et al. 2008; Searle et al. 2009a; Searle et al. 2009b; Gabriel et al. 2011; Macholán et al. 2012; Jones et al. 2013; Li et al. 2021). The house mouse exhibits high morphological and genetic diversity, with three main subspecies recognized: *M. musculus castaneus*, *M. m. musculus*, and *M. m. domesticus* (Boursot et al. 1996; Salcedo et al. 2007; Phifer-Rixey et al. 2020; Fujiwara et al. 2022a). These subspecies diverged around 180–500 kya and underwent secondary contact after dispersing from their native habitat around South Asia (Boursot et al. 1993; Din et al. 1996) with asymmetric hybrid incompatibility; the subspecies *domesticus* shows relatively strong hybrid incompatibility with the other two subspecies (White et al. 2011; White et al. 2012). Despite partial reproductive isolation between subspecies, genetic studies have revealed a non-negligible amount of gene flow, and occasional identification of hybrid genotypes (Orth et al. 1998; Ďureje et al. 2012; Fujiwara et al. 2022a). Studying the genetic differentiation and hybridization patterns in *M. musculus* thus provides a unique opportunity to gain insights into human history and the genetic architecture of hybridization among genetically distinct subspecies of a well-studied model organism.

In East Asia, two major subspecies have been widely observed: the subspecies *castaneus* is distributed in southern China and Taiwan, and the subspecies *musculus* is distributed in northern China, the Korean Peninsula, and the Russian Far East (Din et al. 1996; Jing et al. 2014; Fujiwara et al. 2022a). Another subspecies, *M. m. molossinus*, has been recognized in the Japanese archipelago, where researchers have shown through genetic analysis that it is derived from a hybrid between the subspecies *castaneus* and *musculus* (Yonekawa et al. 1980; Yonekawa et al. 1982; Yonekawa et al. 1988; Sakai et al. 2005; Takada et al. 2013), while most wild Japanese house mice predominantly have the genetic background of the subspecies

musculus (Fujiwara et al. 2022a). Mitochondrial haplogroups representing the subspecies *castaneus* are mainly distributed in northern Japan, whereas mitochondrial haplogroups representing the subspecies *musculus* are observed in southern Japan (Terashima et al. 2006; Kuwayama et al. 2017; Li et al. 2021), leading to the hypothesis that the subspecies *castaneus* was introduced from southern China to the Japanese archipelago and *musculus* was introduced from the Korean Peninsula along with the wet-rice field cultivation system (Terashima et al. 2006; Kuwayama et al. 2017). This hypothesis would be similar to the well-known model of the origin of the modern Japanese population, called the dual structure model by Hanihara (1991). The dual structure model assumes that the genetic makeup of the modern Japanese population has been composed of both indigenous Jomon hunter-gatherers and newly migrated Yayoi rice farmers (Hanihara 1991). Recent genetic analyses of modern and ancient human genome studies have revealed that the Jomon originated from one of the basal East Asian populations (McColl et al. 2018; Kanzawa-Kiriyama et al. 2019; Gakuhari et al. 2020; Osada and Kawai 2021). Despite the progress in genomic research in humans, studies into the demographic history of *M. musculus* in East Asia using a genome-wide dataset have not been performed.

Although the genetic diversity of maternally-inherited mitochondrial haplotypes in wild house mice has been well studied, natural variation in the paternally-inherited Y Chromosome has remained largely unknown, except for a few examples (Morgan and Pardo-Manuel de Villena 2017). Recent experimental studies have discovered X- and Y-linked loci that are crucial for hybrid incompatibility, where copy number variation plays a significant role in determining hybrid incompatibility and sex-ratio distortion (SD). Previous studies have demonstrated that Y-linked *Sly* suppresses post-meiotic expression of X- and Y-linked genes in sperm (Ellis et al. 2011; Cocquet et al. 2012). A copy number increase in *Sly* results in male-biased progenies, while a copy number increase in X-linked *Slx1* counteracts this (Scavetta and Tautz 2010; Cocquet et al. 2012). Morgan and Pardo-Manuel (2017) showed that the

subspecies *musculus* tended to have higher *Sly*/*Slx* copy numbers than other subspecies, but their analyzed samples were biased toward wild-derived inbred lines (Morgan and Pardo-Manuel de Villena 2017). Therefore, the analysis of copy number variations of *Sly*/*Slx* and their natural distribution range in wild samples would provide insight into how the SD alleles affect the genetic differentiation of mouse subspecies.

The selective forces on the formation of hybrid genomes are also an important issue in evolutionary biology research. With the advancement of genome sequencing technology, many genome-scale studies have been conducted to examine the effects of natural selection under interspecific or intersubspecific gene flow. In particular, adaptive gene introgression, in which beneficial alleles cross the boundary of populations and spread rapidly to another population, has attracted the interest of many researchers (Song et al. 2011; Pardo-Diaz et al. 2012; Huerta-Sánchez et al. 2014; Enard and Petrov 2018). The distinctive genetic characteristics of wild Japanese house mice would provide a great opportunity to investigate the effects of selection during hybridization. Having the major genetic background of the subspecies *musculus*, the preference for the genomic region of *castaneus*-ancestry in the Japanese population leaves a similar signature to that of adaptive introgression and is a robust signal of natural selection during hybrid genome formation.

In this study, we analyze 163 high-coverage whole genome sequences of *M. musculus*, including newly sequenced samples primarily from Japan, to quantify the pattern of genetic admixture among the samples. By contrasting the population differentiation patterns of autosomal and sex-linked genomic regions, we infer the evolutionary history of the two East Asian subspecies populations. We also analyze Japanese samples to identify specific regions of the genome where genetic components from the subspecies *castaneus* are more prevalent, even though the majority of the Japanese samples have a genetic background from the subspecies *musculus*. Focusing on the evolutionary history of *M. musculus* in East Asia, this study provides

new insights into how this commensal animal has shaped its genetic traits through secondary contact mediated by human activities.

Results

Genome-wide pattern of differentiation in East Asia

In this study, we sequenced the genome of 37 wild house mice mainly collected from Japan, with an average coverage of 26.3 (Supplemental Table S1). Those data were merged with a previously published dataset that included *Mus spretus*, yielding the genotypes of 170 samples. After filtering, 133,886,237 autosomal biallelic single nucleotide variants (SNVs) were used for the initial population study (Supplemental Method 1).

Principal component analysis (PCA) was performed on all *M. musculus* samples (Supplemental Fig. S1). The results were in high agreement with those previously reported by Fujiwara *et al*. (2022). Three major genetic components corresponding to subspecies *castaneus*, *domesticus*, and *musculus*, were observed. Most of the East Asian samples aligned on the *castaneus-musculus* cline, which means that the genetic characteristics of the East Asian samples can be modeled by different degrees of admixture between the subspecies *castaneus* and *musculus*. Genetic clustering was performed using ADMIXTURE software assuming three ancestral populations (K = 3). The results yielded three genetic components corresponding to the three main subspecies, consistent with the PCA results (Supplemental Fig. S2).

To quantify the degree of genetic admixture in each sample, the f_4-ratio value developed by Patterson *et al*. (2012) was calculated for each sample (see Methods), assuming that the East Asian samples were derived from an admixture of two unknown lineages that shared ancestry with the Korean *musculus* and Indian *castaneus* populations. The estimated percentage of *musculus* ancestry, expressed as α, varied from 0.109 to 1 among the East Asian samples, as shown in Fig. 1. In the Japanese archipelago, all samples had α values greater than 0.564, and the mean value of α was 0.878 (Fig. 1). The samples from the Sea of Japan side have lower α values than those from the Pacific Ocean side. When the sample from Okinawa (a subtropical

island) was excluded and the other samples were divided into two classes according to the Central Watershed of Japan, the Pacific-side samples had significantly higher α values than the Sea of Japan-side samples (P = 0.0002, Mann–Whitney U test). In China, α values were close to 1 in northern and western regions, but were much lower in southern China (Fig. 1). In the southern Chinese samples, the average α value was 0.295, indicating that the genetic background of southern Chinese samples is mostly derived from the subspecies *castaneus*.

Genetic differentiation at mitochondrial genome and sex chromosomes

We compared genetic differentiation patterns at autosomal, X-chromosomal, Y-chromosomal, and mitochondrial loci. We observed generally less mixing of subspecies genomes on the X Chromosome; *i.e.*, there was less *castaneus*-ancestry in the Japanese population and less *musculus*-ancestry in the southern Chinese population on the X Chromosomes. The estimated α values on the X Chromosome ranged from 0.317 to 1 (average α: 0.860) for Japanese samples and from 0.034 to 0.952 (average α: 0.207) for southern Chinese samples, showing that the X Chromosome has a low level of introgression into the predominant genome. The differences in α value between autosomes and X Chromosomes were significant in both Japanese (P = 0.0008) and southern Chinese (P = 0.0134) populations (Wilcoxon signed rank test).

The genealogies of the mitochondrial and Y-chromosomal loci inferred by the maximum-likelihood method (Supplemental Method 2) are shown in Supplemental Figs. S3 and S4, respectively. The Y-chromosomal locus formed three distinct haplogroups corresponding to the three major subspecies, whereas the mitochondrial locus showed five major haplogroups. In addition to the three mitochondrial haplogroups representing the subspecies *castaneus*, *domesticus*, and *musculus*, samples from Madagascar and Nepal formed distinct mitochondrial haplogroups, as previously shown (Fujiwara et al. 2022a; Fujiwara et al. 2022b).

Mitochondrial genomes of the samples were reconstructed through de novo assembly

(detailed in Supplemental Method 3), and their phylogeographic patterns were then compared with those observed in the Y Chromosomes. The geographic distribution of the subspecies *castaneus*- and *musculus*-type haplotypes was markedly different between mitochondrial and Y-chromosomal loci (Fig. 2). The distribution of mitochondrial haplotypes was consistent with previous findings (Fig. 2A); in the Japanese archipelago, *castaneus*- and *musculus*-type mitochondrial haplotypes are distributed in the northern and southern regions of mainland Japan, respectively. In China, the distribution of mitochondrial haplotypes was clearly divided around the Yangtze River basin (or divided at the Qinling Mountains), with *musculus*-type haplotypes in northern China and *castaneus*-type haplotypes in southern China. However, all Y-chromosomal haplotypes in East Asia were assigned exclusively to *musculus*-type haplotypes (Fig. 2B). The Y Chromosome of the reference genome (C57BL/6J) also had a *musculus*-type haplotype, and it was closely related to the haplotype of Japanese samples from the Tohoku area (Supplemental Fig. S4), supporting the idea that the Y Chromosome of classical inbred strains originated from Japanese house mice (Japanese fancy mouse) (Bishop et al. 1985; Nagamine et al. 1992; Tucker et al. 1992; Takada et al. 2013).

We hypothesized that the dominance of the *musculus*-type Y Chromosome in East Asia is due to a distorted sex ratio caused by a dosage imbalance in the *Sly*/*Slx* genes; *Sly* and *Slx* are gametologs under X-Y sexual conflict and are highly duplicated genes (>100 copies). Previous studies have shown that *musculus*-type Y Chromosomes encompass more *Sly* copies and the subspecies *musculus* have more copies of *Slx* on the X Chromosome (Morgan and Pardo-Manuel de Villena 2017). Estimating the copy numbers of *Sly* and *Slx*, however, is challenging due to the presence of highly similar but distinct classes of repetitive sequences in the genome. To tackle this, we first aligned the paralogous sequences of the *Sly* and *Slx* loci present in the reference genome and used these alignments to reconstruct a phylogenetic tree. The reconstructed tree showed two clusters for *Slx*, which correspond to *Slx* (X1) and *Slxl1* (X2),

and six clusters for *Sly* (Y1–Y6), with one cluster (Y1) being the most abundant in the reference genome and including the canonical *Sly* (Fig. 3A). We then estimated copy numbers for each cluster based on the short-read depth of cluster-specific SNV alleles (see Methods). We observed that different subspecies-level Y haplotypes harbored different patterns of *Sly* clusters (Fig. 3B). Cluster Y5 was the major cluster in the *castaneus*-type haplotypes, while cluster Y1 was the major cluster in the *domesticus*-type and *musculus*-type Y haplotypes. Particularly, *castaneus*- and *domesticus*-type Y haplotypes had low *Sly* copy numbers, while *musculus*-type Y haplotypes had high copy numbers among the three haplogroups. By contrast, the copy number ratios of *Slx* and *Slxl1* were mostly consistent among samples. As shown in Fig. 3B, Supplemental Fig. S5, and the previous study, *Sly* and *Slx* copy numbers in the same male individuals were highly correlated ($P < 10^{-22}$, Spearman's rank correlation test) (Morgan and Pardo-Manuel de Villena 2017).

It's remarkable that the southern Chinese population predominantly shares a genetic background with the subspecies *castaneus*, yet exclusively carries Y Chromosomes from the subspecies *musculus*. To explore the selective pressures driving this distinct pattern of Y Chromosome haplotypes in southern China, we conducted Wright–Fisher model simulations. The model assumes that a small fraction of the subspecies *musculus* individuals with longer haplotypes of the SD locus on the sex chromosomes (corresponding to *Sly* and *Slx*) migrate to the subspecies *castaneus* population at a constant rate, *Nm*, where *N* and m represent effective population size and the migratory fraction of individuals per generation, respectively. An F1 hybrid between a subspecies *musculus* male and a subspecies *castaneus* female tend to have more male offspring than female offspring owing to the segregation distortion of X/Y Chromosomes in a male germline. Detailed methods and results are documented in Supplemental Note 1, Supplemental Figs. S6–S10, and Supplemental Table S2.

Briefly, without assuming mutations on copy numbers at the SD locus, the simulations

showed that the introgressed Y Chromosomes with longer SD haplotypes (corresponding to the *musculus*-type *Sly*/*Slx* haplotypes) spread in the recipient population within 0.1*N* generations even with a 10%–20% increase in the male-to-female birth ratio (Supplemental Fig. S6A). Without the SD effect, there is little chance for the introgressed alleles to be fixed in the recipient population within 0.1*N* generation with the assumed migration rate (Nm = 1). The X Chromosomes with longer SD haplotypes also eventually fix in the recipient population; however, the fixation of longer SD haplotypes was in general much faster on the Y Chromosomes than on the X Chromosomes because we assume that SD occurs on the male germline.

We also investigate the effect of hybrid incompatibility between different genomes, including the incompatibility between autosomes, between autosomes and X Chromosomes, and between autosomes and mitochondrial genomes (Presgraves 2008; Bonnet et al. 2017; Fraïsse and Sachdeva 2020; Healy and Burton 2020). In particular, the incompatibility between autosomes and X Chromosomes would be highly likely given that we observed less introgression of X Chromosomes than autosomes in the two hybrid populations, Japanese and southern Chinese populations, with different directions of introgression. The difference in fixation time between the introgressed Y and X Chromosomes becomes longer when the effect of the X-chromosomal hybrid incompatibility (XHI). When the effect of XHI is sufficiently strong, the introgression of X Chromosomes with longer SD haplotypes is completely suppressed (Supplemental Fig. S7C).

Selection during admixture in the Japanese population

To identify genomic regions affected by natural/sexual selection during intersubspecific admixture, we focused on samples from the Japanese archipelago and searched for genomic regions highly enriched in *castaneus*-ancestry haplotypes. Following the results presented in Fig. 1, we estimated the values of α, representing the proportion of *musculus*-like genomic components, for each non-overlapping 20-kb-long window of the autosomal genome.

To discern the neutral distribution of *castaneus*-enriched genomic blocks within the Japanese house mouse population, we employed Fastsimcoal2 software (Excoffier et al. 2013) and inferred demographic parameters from our sample set (See Supplemental Note 2, Supplemental Figs. S9 and S10, and Supplemental Table S3 for details). Using the estimated demographic parameters, we executed 200,000 coalescent simulations to draw a distribution of α under neutrality. From our results, we identified 2,655 outlier windows. These windows, which fell below the 5% threshold of the neutral distribution, encompassed the protein-coding regions of 842 distinct genes. A comprehensive list of these genes can be found in Supplemental Table S4.

We first tested the correlation between the *castaneus*-enriched windows with the gene density and recombination rate. The *castaneus*-enriched windows in the Japanese samples showed significant depletion of genes ($P < 10^{-5}$, chi-square test), as well as a significantly lower recombination rate ($P < 10^{-12}$, Mann–Whitney *U* test), compared with the genomic background (Supplemental Fig. S11). We further performed functional enrichment analysis on the 842 candidate genes using MetaScape software (Zhou et al. 2019). A total of 20 gene categories were found to be enriched in the list (*P* values < 0.01), with the complete list of significantly overrepresented functional categories presented in Supplemental Fig. S12. The enriched term list contained a variety of gene categories, but notably, immune-related gene categories such as immunoglobulin production (GO:002377), antibody-dependent cellular cytotoxicity (GO:0001788), and herpes simplex virus 1 infection (mmu05168) were overrepresented. Indeed, our screening accurately identified the retroelement-like *Fv1* (Friend virus susceptibility protein 1) gene, an antiviral factor (Best et al. 1996), as a *castaneus*-ancestry enriched gene in Japan. Previous studies have demonstrated that the $Fv1^b$ allele, which lacks the 1.3-kb deletion commonly found in the subspecies *domesticus* and *musculus*, is observed with high frequency in the subspecies *castaneus* and Japanese samples (Boso et al. 2021). We confirmed that the deletion started from Chr4:147,870,288 (GRCm38) and was 1.2 kb in length, resulting in

truncation of the C-terminal region of *Fv1* (Supplemental Method 4). The allele frequencies for the deletion were 0.92, 0.64, and 0.16 in the subspecies *domesticus*, *musculus*, and *castaneus*, respectively. The allele frequency in the Japanese samples was 0.02, showing that almost no Japanese house mice harbor the deletion.

We also observed that 23 vomeronasal receptor genes (*Vmn1r* and *Vmn2r*), including one pseudogene, were present in the gene list. In the enrichment analysis, one particular category, detection of chemical stimulus involved in sensory perception (GO0050907), showed the strongest bias (Supplemental Fig. S12). These *castaneus*-enriched vomeronasal receptor genes were scattered across different olfactory/vomeronasal genomic clusters on the mouse genome, with most genes located in a large cluster on Chromosome 7: region Chr7:84,853,553–87,037,968, containing 17 olfactory and 15 vomeronasal receptors. Of the 23 vomeronasal receptor genes identified in our genomic scan, 12 were located in the cluster. For illustration purposes, we present the segregation pattern of SNVs in the *Vmn2r65* and *Vmn2r70* genes residing in this cluster (Fig. 4). These examples distinctly demonstrate that the Japanese samples exhibit a closer genetic affinity to the subspecies *castaneus* than to the subspecies *musculus* in these regions. To confirm that the estimated low α in the region was not due to errors in statistical inference, we computed the F_{ST} between Japanese and subspecies *musculus* samples ($F_{ST\text{-}MUS/JPN}$) and the F_{ST} between Japanese and subspecies *castaneus* samples ($F_{ST\text{-}CAS/JPN}$). The subspecies *castaneus* and *musculus* samples were assigned from the result of the ADMIXTURE analysis. We plotted window-averaged $F_{ST\text{-}CAS/JPN}$ and $F_{ST\text{-}MUS/JPN}$ values across the region including Chr7:84,853,553–87,037,968 (Fig. 5). As expected, outside of this region, the $F_{ST\text{-}MUS/JPN}$ values were consistently smaller than the $F_{ST\text{-}CAS/JPN}$ values, supporting the notion that Japanese samples were generally *musculus*-like. However, the pattern was completely reversed within the olfactory/vomeronasal clusters, indicating an unusual pattern of genetic admixture in this region. We also estimated genealogies around the target nonsynonymous SNVs of the

289 *Vmn2r* genes using RELATE software (Speidel et al. 2019) (Supplemental Method 5). The
290 genealogies encompassing *Vmn2r65* and *Vmn2r70* showed that the *castaneus*-type Japanese
291 alleles coalesced with the other *castaneus*-type alleles after the split of the subspecies *castaneus*
292 and *musculus*, which was estimated to occur around 200 kya from our data (Fig. 4).

Discussion

Genetic differentiation and inferred history of M. musculus in East Asia

The widespread coexistence of the subspecies *castaneus* and *musculus* in East Asia suggests that they formed a broad hybrid zone following their initial migration from their homeland. Previous studies have inferred migration scenarios primarily based on phylogeographical patterns of mitochondrial genomes (Jing et al. 2014; Li et al. 2021). We present a combined view from autosomal, mitochondrial, X-chromosomal, and Y-chromosomal loci result in Supplemental Note 3.

Spread of musculus-type Y Chromosomes in East Asia

In this study, we uncovered natural variation in the Y Chromosomes of house mice across Eurasia, identifying distinct clusters corresponding to major subspecies. All Y Chromosomes in East Asian samples were of the *musculus*-type, which could be explained by various mechanisms such as natural/sexual selection (Veltsos et al. 2008; Petr et al. 2020), male-biased migration (Tosi et al. 2003), and genetic drift. Genomic conflict between X and Y Chromosomes offers a plausible explanation for such biased transmission, as suggested in species such as *Drosophila* (Branco et al. 2013) and the great apes (Nam et al. 2015). In our specific case, the *Sly*/*Slx* system is likely a major contributor, where SD is well validated by experimental evidence.

In the *Sly*/*Slx* system, the subspecies *musculus* possesses longer, and thus potentially more advantageous, haplotypes for both the X and Y Chromosomes. This genetic advantage should theoretically expedite the introgression of both chromosome types but at different magnitudes. Our computer simulations indicated faster fixation of *musculus*-type Y Chromosomes compared with *musculus*-type X Chromosomes, even in the absence of other factors. However, when considering hybrid incompatibility between genomes, particularly between autosomes and X

Chromosomes as well as autosomes and mitochondrial genomes, the rate of introgression for *musculus*-type X Chromosomes was significantly reduced (Supplemental Fig. S7 and Supplemental Table S2). Previous research has highlighted the significance of both autosomal-X chromosomal (Presgraves 2008; Fraïsse and Sachdeva 2020) and autosomal-mitochondrial hybrid incompatibilities (Bonnet et al. 2017; Healy and Burton 2020), supported by both experimental and theoretical evidence. We thus propose that these factors also play a crucial role in the pronounced difference in introgression patterns between X and Y Chromosomes observed in southern China.

Post-admixture natural selection in the Japanese archipelago

Detecting the signatures of natural selection during genetic admixture is an important yet challenging topic in evolutionary biology. This challenge arises because, following admixture or introgression, it is typically the pre-existing alleles (i.e., standing variation) rather than new mutations that are subject to selection. Traditional methods for detecting selective sweeps generally focus on hard sweeps driven by new mutations. By contrast, post-admixture positive selection often manifests as soft sweeps, which are statistically more difficult to detect (e.g., (Hermisson et al. 2017). The unique genetic composition of Japanese house mice presents an excellent opportunity to robustly investigate selection signatures, demonstrating the complexity of evolutionary processes at play.

To establish thresholds for identifying *castaneus*-enriched genomic regions within Japanese populations, we estimated demographic parameters using Fastsimcoal2 (see Supplemental Note 2 and Supplemental Fig. S9). Despite the agreement between expected and observed site frequency spectra after parameter optimization in the Japanese population (Supplemental Fig. S10), caution is advised when interpreting parameters derived from Fastsimcoal2 because of the model's inherent limitations. Consequently, the representation of *castaneus*-enriched windows may not be entirely accurate. Nonetheless, a robust and discernible pattern among these

342 windows suggests the influence of natural selection. Notably, we observed a significant
343 reduction in gene density and recombination rates within *castaneus*-enriched windows,
344 indicating the role of negative selection in purging introgressed alleles, aligning with
345 observations from studies on human-Neanderthal admixtures (Sankararaman et al. 2014).
346 Although these windows are outliers within a neutral framework, many *castaneus*-type alleles in
347 these regions likely increase in frequency due to genetic drift. In particular, a decrease in local
348 effective population size due to reduced recombination rates enhances the likelihood of
349 introgressed alleles achieving high frequency within a recipient population. Nevertheless, the
350 prevalence of immune-related and olfactory-related genes within these windows points towards
351 their positive selection, hinting at their adaptive significance despite the overarching negative
352 selection pressure.

353 Genes involved in host defense mechanisms were significantly enriched in the outlier loci. In
354 the case of humans, several studies have shown evidence of adaptive introgression from archaic
355 to modern humans at immune-related loci (Racimo et al. 2015; Enard and Petrov 2018). For
356 example, we identified *Irgm1* and *Irgm2*, which are GTPases involved in the interferon
357 signaling pathway, in our candidate list. In particular, *Irgm2* has been shown to be responsible
358 for defense against *Toxoplasma*, and several *castaneus*-type tightly-linked nonsynonymous
359 SNVs were common among the Japanese samples (Supplemental Figs. S13 and S14). In another
360 example, the *castaneus*-ancestry enriched regions contained six cathepsin genes on
361 Chromosome 13. Two of them, *Ctsj* and *Ctsr*, are exclusive to the adult placenta, and may be
362 responsible for the process of viral infection. Although the roles of *Ctsj* and *Ctsr* in viral
363 infection have yet to be demonstrated, maternal–fetal viral transmission might be a critical
364 factor during the process of hybrid formation. Alternatively, these placental genes may be
365 responsible for the compatibility between the genotypes of mother and offspring.

366 In addition to these genes, vomeronasal receptors exhibited a strongly biased pattern of

segregation. These receptors are expressed in the vomeronasal organ and form a large receptor family involved in vomeronasal chemosensation (Wynn et al. 2012). They recognize a wide variety of chemical cues, such as pheromones from different sexes and predator odors (Dulac and Torello 2003). In some vomeronasal receptor genes, most Japanese samples harbor *castaneus*-type nonsynonymous alleles. Although certain vomeronasal receptor genes are highly differentiated between house mouse subspecies and could serve as markers for discrimination (Wynn et al. 2012), our genealogical analysis revealed that the target genes might have frequently crossed subspecies boundaries (Fig. 4). Furthermore, we noted a concentration of mutations along the branch that differentiates the *castaneus*- and *musculus*-type haplotypes of *Vnm2r70* (Fig. 4). This clustering suggests the influence of positive selection in driving the diversification of these haplotypes. It is thus possible that some vomeronasal alleles become adaptive in other subspecies and quickly spread following introgression. Frequent introgression of olfactory and other chemosensory receptor genes has been observed in the analysis between the subspecies *domesticus* and *musculus* (Staubach et al. 2012; Janousek et al. 2015).

The identified vomeronasal receptors were primarily clustered in a region on mouse Chromosome 7, Chr7:84,853,553–87,037,968. This entire ~2 Mbp region displayed a strongly biased pattern of *castaneus*-ancestry (Fig. 5). Previous extensive studies revealed that *Vmn2r* genes in this cluster respond to cues from conspecific mating partners (Isogai et al. 2011). Detailed studies, such as gene replacement experiments, will elucidate how different vomeronasal receptor alleles contribute to the formation of natural house mouse hybrids in the future.

In this study, we have elucidated the genomic landscape of wild house mice in East Asia. In East Asian house mouse populations, which experienced secondary contact after the subspecies diverged, we have inferred the effects of natural/sexual selection and genomic conflict from the observed pattern of genetic structure at various genomic loci. These findings pave the way for

392 future studies on genetic admixtures between different house mouse subspecies and provide
393 insight into the genetic architecture of hybrid genomes.

Methods

Genomic samples

We sequenced the whole genomes of 37 *M. musculus* samples, and used mitochondrial DNA sequences published in previous studies (Moriwaki et al. 1986; Suzuki et al. 2004; Terashima et al. 2006; Nunome et al. 2010; Suzuki et al. 2013; Kodama et al. 2015; Kuwayama et al. 2017). We combined these data with the global sample dataset used in our prior research (Fujiwara et al. 2022a). A detailed list of these samples can be found in Supplemental Table S1. In total, our analysis included 163 *M. musculus* and 7 *M. spretus* samples. The method for SNV genotyping is presented in Supplemental Note 4.

Population genetics analysis

We conducted PCA on 163 *M. musculus* samples to investigate the population structure. This analysis was performed using smartpca from the Eigensoft software with default parameters, except that outliers were not excluded (Patterson et al. 2006).

To further analyze population structure and the admixture, we employed ADMIXTURE with the number of clusters $K = 3$ for the 163 *M. musculus* samples. Before admixture inference, we pruned SNVs under linkage disequilibrium (LD) using PLINK with the option "--indep-pairwise 50 5 0.5". In downstream analyses, the majority of ancestral proportions determined by ADMIXTURE analysis define the subspecies of each sample.

To quantify the fraction of genomes contributed by the subspecies *musculus* (α) in the East Asian samples, we estimated f_4-ratio statistics (Patterson et al. 2012). The estimation of f_4 statistics was carried out using the "patterson_d" function in the Scikit-allel Python package. Assuming the source of *musculus* genomic components was more closely related to the Korean *musculus* samples than to Kazakh *musculus* samples, we estimated the α value for sample X according to equation (1):

$$\hat{\alpha} = \frac{f_4(KAZ,SPR;X,IND)}{f_4(KAZ,SPR;KOR,IND)} \qquad (1)$$

where KAZ, SPR, KOR, and IND represent the samples from Kazakhstan (5 samples), *M. spretus* (7 samples), Korea (9 samples), and India (2 samples from Leh), respectively. In this scenario, sample X acquires a portion of its genome from the subspecies *musculus* (α) and the remaining proportion (1−α) from the subspecies *castaneus.* Note that while the f_4-ratio statistics allows us to infer the mixing proportions of an admixture event, it cannot determine the direction of introgression. The model is also presented in Supplemental Fig. S9. In principle, α is equal to or smaller than 1, but it may slightly exceed 1 because of statistical fluctuation. When $\alpha > 1$, we set α to 1. Additionally, we estimated the value of α for each 20 kb-length window for all Japanese samples. To remove unreliably estimated values, we excluded windows with fewer than 100 SNVs. Both the denominator and numerator of the right side of equation 1 are expected to be positive, considering that the Japanese and Korean samples are genetically closer to the subspecies *musculus* (KAZ samples) than to the subspecies *castaneus* (IND samples). However, a small fraction of windows showed negative denominators and/or numerators as a result of statistical errors, introgression, or ancestral polymorphisms. Such windows were filtered out from the following analysis. F_{ST} was estimated using the "hudson_fst" function in Scikit-allel.

Copy number estimation of Sly/Slx

We downloaded all of the paralogous sequences of *Sly* (ENSMUSG00000101155) and *Slx* (ENSMUSG00000095063) on the sex chromosomes, including introns, from Ensembl Release 102. The sequences were then aligned using MAFFT (Katoh et al. 2002; Katoh and Standley 2013). Following the alignment, we reconstructed a phylogenetic tree using MEGA X software (Kumar et al. 2018), employing a maximum-likelihood method with the general time reversible (GTR) model. From this alignment, we identified tag-SNV sites with cluster-specific alleles.

We started by mapping the short reads from samples to either *Sly* or *Slx* genomic sequences, incorporating 1000-bp-length flanking sequences for both ends. The copy numbers for each cluster were then estimated by counting the depth of cluster-specific alleles at the tag-SNV sites, using the pileup format files generated from the SAMtools mpileup command. To filter out results from repetitive sequences that might complicate our analysis, we focused solely on sites with a mappability score of 1 (Supplemental Method 1), calculated using autosomal sequences and either *Sly* or *Slx* sequences. To ensure the accuracy and relevance of our results, a filter was applied to exclude sites that exhibited a depth smaller than 1/3 or larger than three times the median. Finally, we estimated the copy number for each sample from the mean depth, which was then divided by half the average depth of the whole genome for the sample.

Data access

All raw short-read sequencing data generated in this study have been submitted to the DNA Data Bank of Japan (DDBJ) DDBJ Sequence Read Archive (DRA) database under accession number PRJDB16017. All complete mitochondrial sequences generated in this study have also been submitted to the DDBJ under accession numbers LC772928–LC772964. The data sets, parameterization files, and scripts required to reproduce the analysis are submitted as Supplemental Data and deposited in the Dryad digital repository (https://datadryad.org/) under doi: https://doi.org/10.5061/dryad.9p8cz8wnb.

Competing interests

The authors declare that they have no competing interests

Acknowledgments

We would like to express our sincere gratitude to the late Dr. Kazuo Moriwaki for collecting valuable wild house mouse samples from around the world. We thank the members of the Yaponesian Genome project funded by MEXT KAKENHI, for their valuable comments and

466 feedback on our research. We are grateful for the insightful feedback provided by three
467 anonymous reviewers. This work was supported by MEXT KAKENHI (grants 18H05511 and
468 23H04846 to N. O. and grant 18H05508 to H. S.). We thank Edanz (https://jp.edanz.com/ac) for
469 editing a draft of this manuscript.

Figure legends

Fig. 1: Estimated ratio of *musculus/castaneus* ancestry in East Asia

The colors of circles indicate the *musculus*/*castaneus* ancestry of samples at each collection site (left panel: East Asian samples except for the Japanese archipelago, right panel: Japanese archipelago samples). The *musculus* ancestry and *castaneus* ancestry of each sample are represented by a range of colors from white to green, with the stronger green color indicating higher *castaneus* ancestry. The range of the ancestry ratio is indicated by the color bar in each panel. The pink line in right panel represents the Central Watershed in the Japanese archipelago.

Fig. 2: Geographic distribution of the subspecies *castaneus* and *musculus* haplotypes of mitochondrial and Y-chromosomal loci

The upper panel (A) and lower panel (B) show the mitochondrial and Y-chromosomal haplotypes, respectively. The colors of circles indicate subspecies haplotypes based on genotyping: *castaneus*-type (green), *domesticus*-type (blue), *musculus*-type (red), and the geographically confined group of Nepalese-type (purple).

Fig. 3: Copy number evolution of *Sly* and *Slx*

The phylogenetic tree of *Sly*/*Slx* genes on the mouse reference genome, GRCm38 (A). Bootstrap values are described at each node. Estimated copy numbers of *Sly* and *Slx* for each sample (B). Different colors represent the copy numbers of different clusters. The samples were aligned according to the subspecies group of Y Chromosome haplotypes first, and sorted ascendingly by the total copy numbers of *Sly* within the groups.

Fig. 4: Haplotype structure of nonsynonymous SNVs and the genealogies of wild house mouse *Vmn2r65* and *Vmn2r70*

The upper panels show the segregation pattern of nonsynonymous SNVs. The sites in the red rectangles represent the focal sites. The lower panels show the inferred genealogies around the focal sites. The blue dots indicate mutations on branches. The branches with the

derived mutations at the focal sites are colored in red. The labels of the samples are shown at the bottom of the tree.

Fig. 5: Distribution of F_{ST} in 20 kb-length windows on Chromosome 7

The yellow and green lines indicate F_{ST} between the Japanese and subspecies *musculus* samples and F_{ST} between the Japanese and subspecies *castaneus* samples, respectively. The lower panel shows the pattern in the olfactory/vomeronasal genes in this cluster (Chr7:84,853,553–87,037,968, GRCm38).

References

Best S, Tissier PL, Towers G, Stoye JP. 1996. Positional cloning of the mouse retrovirus restriction gene Fvl. *Nature* **382**: 826-829.

Bishop CE, Boursot P, Baron B, Bonhomme F, Hatat D. 1985. Most classical Mus musculus domesticus laboratory mouse strains carry a Mus musculus musculus Y chromosome. *Nature* **315**: 70-72.

Bonnet T, Leblois R, Rousset F, Crochet P-A. 2017. A reassessment of explanations for discordant introgressions of mitochondrial and nuclear genomes. *Evolution* **71**: 2140-2158.

Boso G, Lam O, Bamunusinghe D, Oler AJ, Wollenberg K, Liu Q, Shaffer E, Kozak CA. 2021. Patterns of Coevolutionary Adaptations across Time and Space in Mouse Gammaretroviruses and Three Restrictive Host Factors. *Viruses* **13**: 1864.

Boursot P, Auffray JC, Britton-Davidian J, Bonhomme F. 1993. The Evolution of House Mice. *Annu Rev Ecol Syst* **24**: 119-152.

Boursot P, Din W, Anand R, Darviche D, Dod B, Von Deimling F, Talwar GP, Bonhomme F. 1996. Origin and radiation of the house mouse: mitochondrial DNA phylogeny. *J Evol Biol* **9**: 391-415.

Branco AT, Tao Y, Hartl DL, Lemos B. 2013. Natural variation of the Y chromosome suppresses sex ratio distortion and modulates testis-specific gene expression in Drosophila simulans. *Heredity* **111**: 8-15.

Cocquet J, Ellis PJI, Mahadevaiah SK, Affara NA, Vaiman D, Burgoyne PS. 2012. A Genetic Basis for a Postmeiotic X Versus Y Chromosome Intragenomic Conflict in the Mouse. *PLoS Genet* **8**: e1002900.

Din W, Anand R, Boursot P, Darviche D, Dod B, Jouvin-Marche E, Orth A, Talwar GP, Cazenave P-A, Bonhomme F. 1996. Origin and radiation of the house mouse: clues from nuclear genes. *J Evol Biol* **9**: 519-539.

Dulac C, Torello AT. 2003. Molecular detection of pheromone signals in mammals: from genes to behaviour. *Nature Reviews Neuroscience* **4**: 551-562.

Ďureje Ľ, Macholán M, Baird SJE, Piálek J. 2012. The mouse hybrid zone in Central Europe: from morphology to molecules. *Folia Zoologica* **61**: 308-318, 311.

Ellis PJI, Bacon J, Affara NA. 2011. Association of Sly with sex-linked gene amplification during mouse evolution: a side effect of genomic conflict in spermatids? *Hum Mol Genet* **20**: 3010-3021.

Enard D, Petrov DA. 2018. Evidence that RNA Viruses Drove Adaptive Introgression between Neanderthals and Modern Humans. *Cell* **175**: 360-371.e313.

Excoffier L, Dupanloup I, Huerta-Sánchez E, Sousa VC, Foll M. 2013. Robust Demographic Inference from Genomic and SNP Data. *PLoS Genet* **9**: e1003905.

Fraïsse C, Sachdeva H. 2020. The rates of introgression and barriers to genetic exchange between hybridizing species: sex chromosomes vs autosomes. *Genetics* **217**.

Fujiwara K, Kawai Y, Takada T, Shiroishi T, Saitou N, Suzuki H, Osada N. 2022a. Insights into *Mus musculus* Population Structure across Eurasia Revealed by Whole-Genome Analysis. *Genome Biol Evol* **14**.

Fujiwara K, Ranorosoa MC, Ohdachi SD, Arai S, Sakuma Y, Suzuki H, Osada N. 2022b. Whole-genome sequencing analysis of wild house mice (Mus musculus) captured in Madagascar.

Genes Genet Syst **97**: 193-207.

Gabriel SI, Stevens MI, Mathias MdL, Searle JB. 2011. Of Mice and 'Convicts': Origin of the Australian House Mouse, *Mus musculus*. *PLOS ONE* **6**: e28622.

Gakuhari T, Nakagome S, Rasmussen S, Allentoft ME, Sato T, Korneliussen T, Chuinneagáin BN, Matsumae H, Koganebuchi K, Schmidt R et al. 2020. Ancient Jomon genome sequence analysis sheds light on migration patterns of early East Asian populations. *Communications Biology* **3**: 437.

Geraldes A, Basset P, Gibson B, Smith KL, Harr B, Yu H-T, Bulatova N, Ziv Y, Nachman MW. 2008. Inferring the history of speciation in house mice from autosomal, X-linked, Y-linked and mitochondrial genes. *Mol Ecol* **17**: 5349-5363.

Gündüz İ, Auffray JC, Britton-Davidian J, Catalan J, Ganem G, Ramalhinho MG, Mathias ML, Searle JB. 2001. Molecular studies on the colonization of the Madeiran archipelago by house mice. *Mol Ecol* **10**: 2023-2029.

Hanihara K. 1991. Dual Structure Model for the Population History of the Japanese. *Japan Review*: 1-33.

Healy TM, Burton RS. 2020. Strong selective effects of mitochondrial DNA on the nuclear genome. *Proceedings of the National Academy of Sciences* **117**: 6616-6621.

Hermisson J, Pennings PS, Kelley J. 2017. Soft sweeps and beyond: understanding the patterns and probabilities of selection footprints under rapid adaptation. *Methods in Ecology and Evolution* **8**: 700-716.

Huerta-Sánchez E, Jin X, Asan, Bianba Z, Peter BM, Vinckenbosch N, Liang Y, Yi X, He M, Somel M et al. 2014. Altitude adaptation in Tibetans caused by introgression of Denisovan-like DNA. *Nature* **512**: 194-197.

Isogai Y, Si S, Pont-Lezica L, Tan T, Kapoor V, Murthy VN, Dulac C. 2011. Molecular organization of vomeronasal chemoreception. *Nature* **478**: 241-245.

Janousek V, Munclinger P, Wang L, Teeter KC, Tucker PK. 2015. Functional organization of the genome may shape the species boundary in the house mouse. *Mol Biol Evol* **32**: 1208-1220.

Jing M, Yu H-T, Bi X, Lai Y-C, Jiang W, Huang L. 2014. Phylogeography of Chinese house mice (*Mus musculus musculus/castaneus*): distribution, routes of colonization and geographic regions of hybridization. *Mol Ecol* **23**: 4387-4405.

Jones EP, Eager HM, Gabriel SI, Jóhannesdóttir F, Searle JB. 2013. Genetic tracking of mice and other bioproxies to infer human history. *Trends Genet* **29**: 298-308.

Kanzawa-Kiriyama H, Jinam TA, Kawai Y, Sato T, Hosomichi K, Tajima A, Adachi N, Matsumura H, Kryukov K, Saitou N et al. 2019. Late Jomon male and female genome sequences from the Funadomari site in Hokkaido, Japan. *Anthropol Sci* **127**: 83-108.

Katoh K, Misawa K, Kuma K, Miyata T. 2002. MAFFT: a novel method for rapid multiple sequence alignment based on fast Fourier transform. *Nucleic Acids Res* **30**: 3059-3066.

Katoh K, Standley DM. 2013. MAFFT multiple sequence alignment software version 7: improvements in performance and usability. *Mol Biol Evol* **30**: 772-780.

Kodama S, Nunome M, Moriwaki K, Suzuki H. 2015. Ancient onset of geographical divergence, interpopulation genetic exchange, and natural selection on theMc1rcoat-colour gene in the house mouse (*Mus musculus*). *Biol J Linn Soc* **114**: 778-794.

Kumar S, Stecher G, Li M, Knyaz C, Tamura K. 2018. MEGA X: Molecular Evolutionary Genetics Analysis across Computing Platforms. *Mol Biol Evol* **35**: 1547-1549.

Kuwayama T, Nunome M, Kinoshita G, Abe K, Suzuki H. 2017. Heterogeneous genetic make-up of Japanese house mice (*Mus musculus*) created by multiple independent introductions

599 and spatio-temporally diverse hybridization processes. *Biol J Linn Soc* **122**: 661-674.

600 Li Y, Fujiwara K, Osada N, Kawai Y, Takada T, Kryukov AP, Abe K, Yonekawa H, Shiroishi
601 T, Moriwaki K et al. 2021. House mouse *Mus musculus* dispersal in East Eurasia inferred from
602 98 newly determined complete mitochondrial genome sequences. *Heredity (Edinb)* **126**: 132-147.

603 Macholán M, Baird SJE, Munclinger P, Piálek J. 2012. *Evolution of the House Mouse*.
604 Cambridge University Press, Cambridge.

605 McColl H, Racimo F, Vinner L, Demeter F, Gakuhari T, Moreno-Mayar JV, van Driem G,
606 Gram Wilken U, Seguin-Orlando A, de la Fuente Castro C et al. 2018. The prehistoric peopling
607 of Southeast Asia. *Science* **361**: 88-92.

608 Morgan AP, Pardo-Manuel de Villena F. 2017. Sequence and Structural Diversity of Mouse Y
609 Chromosomes. *Mol Biol Evol* **34**: 3186-3204.

610 Moriwaki K, Miyashita N, Suzuki H, Kurihara Y, Yonekawa H. 1986. Genetic Features of
611 Major Geographical Isolates of *Mus musculus*. doi:10.1007/978-3-642-71304-0_6 (ed. M Potter,
612 et al.), pp. 55-61. Springer.

613 Nagamine CM, Nishioka Y, Moriwaki K, Boursot P, Bonhomme F, Lau YFC. 1992. The
614 *musculus*-type Y Chromosome of the laboratory mouse is of Asian origin. *Mamm Genome* **3**: 84-
615 91.

616 Nam K, Munch K, Hobolth A, Dutheil JY, Veeramah KR, Woerner AE, Hammer MF, Project
617 GAGD, Mailund T, Schierup MH et al. 2015. Extreme selective sweeps independently targeted
618 the X chromosomes of the great apes. *Proceedings of the National Academy of Sciences* **112**:
619 6413-6418.

620 Nunome M, Ishimori C, Aplin KP, Tsuchiya K, Yonekawa H, Moriwaki K, Suzuki H. 2010.
621 Detection of recombinant haplotypes in wild mice (*Mus musculus*) provides new insights into the
622 origin of Japanese mice. *Mol Ecol* **19**: 2474-2489.

623 Orth A, Adama T, Din W, Bonhomme F. 1998. Natural hybridization between two subspecies
624 of the house mouse, *Mus musculus domesticus* and *Mus musculus castaneus*, near Lake Casitas,
625 California. *Genome* **41**: 104-110.

626 Osada N, Kawai Y. 2021. Exploring models of human migration to the Japanese archipelago
627 using genome-wide genetic data. *Anthropol Sci* **129**: 45-58.

628 Pardo-Diaz C, Salazar C, Baxter SW, Merot C, Figueiredo-Ready W, Joron M, McMillan WO,
629 Jiggins CD. 2012. Adaptive Introgression across Species Boundaries in *Heliconius* Butterflies.
630 *PLoS Genet* **8**: e1002752.

631 Patterson N, Moorjani P, Luo Y, Mallick S, Rohland N, Zhan Y, Genschoreck T, Webster T,
632 Reich D. 2012. Ancient Admixture in Human History. *Genetics* **192**: 1065-1093.

633 Patterson N, Price AL, Reich D. 2006. Population Structure and Eigenanalysis. *PLoS Genet* **2**:
634 e190.

635 Petr M, Hajdinjak M, Fu Q, Essel E, Rougier H, Crevecoeur I, Semal P, Golovanova LV,
636 Doronichev VB, Lalueza-Fox C et al. 2020. The evolutionary history of Neanderthal and
637 Denisovan Y chromosomes. *Science* **369**: 1653-1656.

638 Phifer-Rixey M, Harr B, Hey J. 2020. Further resolution of the house mouse (*Mus musculus*)
639 phylogeny by integration over isolation-with-migration histories. *BMC Evol Biol* **20**: 120.

640 Presgraves DC. 2008. Sex chromosomes and speciation in *Drosophila*. *Trends in genetics :*
641 *TIG* **24**: 336-343.

642 Racimo F, Sankararaman S, Nielsen R, Huerta-Sánchez E. 2015. Evidence for archaic
643 adaptive introgression in humans. *Nature Reviews Genetics* **16**: 359-371.

644 Sakai T, Kikkawa Y, Miura I, Inoue T, Moriwaki K, Shiroishi T, Satta Y, Takahata N,

Yonekawa H. 2005. Origins of mouse inbred strains deduced from whole-genome scanning by polymorphic microsatellite loci. *Mamm Genome* **16**: 11-19.

Salcedo T, Geraldes A, Nachman MW. 2007. Nucleotide Variation in Wild and Inbred Mice. *Genetics* **177**: 2277-2291.

Scavetta RJ, Tautz D. 2010. Copy Number Changes of CNV Regions in Intersubspecific Crosses of the House Mouse. *Mol Biol Evol* **27**: 1845-1856.

Searle JB, Jamieson PM, Gündüz İ, Stevens MI, Jones EP, Gemmill CEC, King CM. 2009a. The diverse origins of New Zealand house mice. *Proceedings of the Royal Society B: Biological Sciences* **276**: 209-217.

Searle JB, Jones CS, Gündüz İ, Scascitelli M, Jones EP, Herman JS, Rambau RV, Noble LR, Berry RJ, Giménez MD et al. 2009b. Of mice and (Viking?) men: phylogeography of British and Irish house mice. *Proceedings of the Royal Society B: Biological Sciences* **276**: 201-207.

Song Y, Endepols S, Klemann N, Richter D, Matuschka F-R, Shih C-H, Nachman Michael W, Kohn Michael H. 2011. Adaptive Introgression of Anticoagulant Rodent Poison Resistance by Hybridization between Old World Mice. *Curr Biol* **21**: 1296-1301.

Speidel L, Forest M, Shi S, Myers SR. 2019. A method for genome-wide genealogy estimation for thousands of samples. *Nat Genet* **51**: 1321-1329.

Staubach F, Lorenc A, Messer PW, Tang K, Petrov DA, Tautz D. 2012. Genome Patterns of Selection and Introgression of Haplotypes in Natural Populations of the House Mouse (*Mus musculus*). *PLoS Genet* **8**: e1002891.

Suzuki H, Nunome M, Kinoshita G, Aplin KP, Vogel P, Kryukov AP, Jin M-L, Han S-H, Maryanto I, Tsuchiya K et al. 2013. Evolutionary and dispersal history of Eurasian house mice *Mus musculus* clarified by more extensive geographic sampling of mitochondrial DNA. *Heredity* **111**: 375-390.

Suzuki H, Shimada T, Terashima M, Tsuchiya K, Aplin K. 2004. Temporal, spatial, and ecological modes of evolution of Eurasian Mus based on mitochondrial and nuclear gene sequences. *Mol Phylogen Evol* **33**: 626-646.

Takada T, Ebata T, Noguchi H, Keane TM, Adams DJ, Narita T, Shin-I T, Fujisawa H, Toyoda A, Abe K et al. 2013. The ancestor of extant Japanese fancy mice contributed to the mosaic genomes of classical inbred strains. *Genome Res* **23**: 1329-1338.

Terashima M, Furusawa S, Hanzawa N, Tsuchiya K, Suyanto A, Moriwaki K, Yonekawa H, Suzuki H. 2006. Phylogeographic origin of Hokkaido house mice (*Mus musculus*) as indicated by genetic markers with maternal, paternal and biparental inheritance. *Heredity* **96**: 128-138.

Tosi AJ, Morales JC, Melnick DJ. 2003. Paternal, maternal, and biparental molecular markers provide unique windows onto the evolutionary history of macaque monkeys. *Evolution* **57**: 1419-1435.

Tucker PK, Lee BK, Lundrigan BL, Eicher EM. 1992. Geographic origin of the Y chromosomes in "old" inbred strains of mice. *Mamm Genome* **3**: 254-261.

Veltsos P, Keller I, Nichols RA. 2008. The Inexorable Spread of a Newly Arisen Neo-Y Chromosome. *PLoS Genet* **4**: e1000082.

White MA, Steffy B, Wiltshire T, Payseur BA. 2011. Genetic Dissection of a Key Reproductive Barrier Between Nascent Species of House Mice. *Genetics* **189**: 289-304.

White MA, Stubbings M, Dumont BL, Payseur BA. 2012. Genetics and Evolution of Hybrid Male Sterility in House Mice. *Genetics* **191**: 917-934.

Wynn EH, Sánchez-Andrade G, Carss KJ, Logan DW. 2012. Genomic variation in the vomeronasal receptor gene repertoires of inbred mice. *BMC Genomics* **13**: 415.

Yonekawa H, Moriwaki K, Gotoh O, Miyashita N, Matsushima Y, Shi LM, Cho WS, Zhen XL, Tagashira Y. 1988. Hybrid origin of Japanese mice "*Mus musculus molossinus*": evidence from restriction analysis of mitochondrial DNA. *Mol Biol Evol* **5**: 63-78.

Yonekawa H, Moriwaki K, Gotoh O, Miyashita N, Migita S, Bonhomme F, Hjorth JP, Petras ML, Tagashira Y. 1982. Origins of laboratory mice deduced from restriction patterns of mitochondrial DNA. *Differentiation* **22**: 222-226.

Yonekawa H, Moriwaki K, Gotoh O, Watanabe J, Hayashi J-I, Miyashita N, Petras ML, Tagashira Y. 1980. Relationship Between Laboratory Mice and the Subspecies *Mus musculus domesticus* Based on Restriction Endonuclease Cleavage Patterns of Mitochondrial DNA. *The Japanese journal of genetics* **55**: 289-296.

Zhou Y, Zhou B, Pache L, Chang M, Khodabakhshi AH, Tanaseichuk O, Benner C, Chanda SK. 2019. Metascape provides a biologist-oriented resource for the analysis of systems-level datasets. *Nat Commun* **10**: 1523.

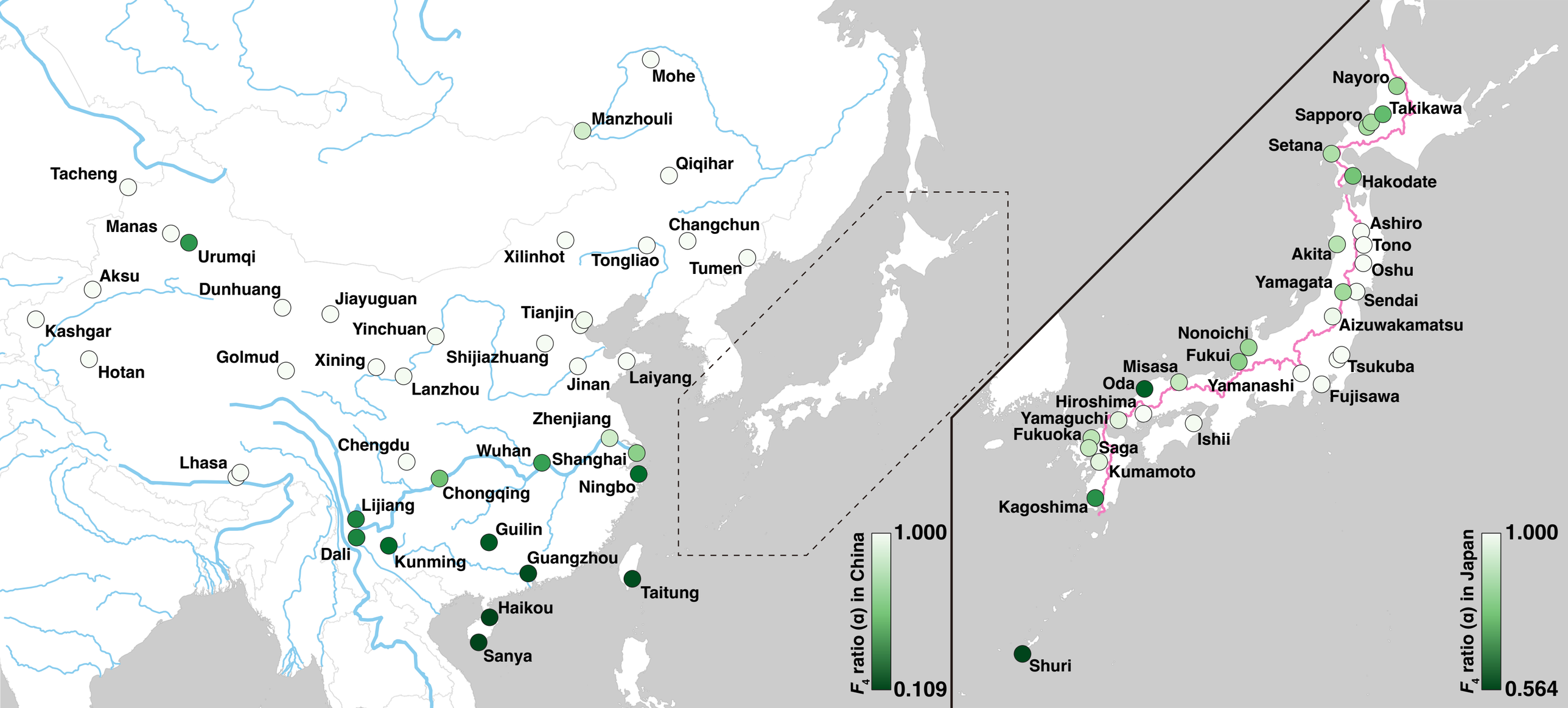
Mohe
Manzhouli
Qiqihar
Tacheng
Changchun
Manas
Urumqi
Xilinhot
Tongliao
Tumen
Aksu
Dunhuang
Jiayuguan
Tianjin
Kashgar
Yinchuan
Golmud
Xining
Shijiazhuang
Hotan
Lanzhou
Jinan
Laiyang
Zhenjiang
Chengdu
Wuhan
Shanghai
Lhasa
Ningbo
Chongqing
Lijiang
Guilin
Dali
Kunming
Guangzhou
Taitung
Haikou
Sanya
Nayoro
Takikawa
Sapporo
Setana
Hakodate
Ashiro
Tono
Akita
Oshu
Yamagata
Sendai
Aizuwakamatsu
Nonoichi
Fukui
Tsukuba
Misasa
Oda
Yamanashi
Fujisawa
Hiroshima
Yamaguchi
Ishii
Fukuoka
Saga
Kumamoto
Kagoshima
Shuri
F_4 ratio (α) in China
1.000
0.109
F_4 ratio (α) in Japan
1.000
0.564

A

Gorno-Altaysk
Irkutsk
Chita
Mohe
Okha
Krementui
Manzhouli
Birakan
Poronaysk
Khabarovsk
Qiqihar
Tacheng
Manas
Changchun
Urumqi
Almaty
Xilinhot
Tongliao
Aksu
Dunhuang
Jiayuguan
Kashgar
Yinchuan
Tianjin
Laiyang
Hotan
Golmud
Xining
Shijiazhuang
Jinan
Lanzhou
Leh
Zhenjiang
Chengdu
Wuhan
Lahore
Himalaya
Shanghai
Lhasa
Chongqing
Ningbo
Delhi
Tukuche
Lijiang
Kathmandu
Mymensingh
Guilin
Dali
Kunming
Guangzhou
Dhaka
Taitung
Lashio
Hanoi
Bhubaneswar
Vinh Phuc
Haikou
Sanya
Hyderabad
Languna
Yuzhno-Sakhalinsk
Rudnaya Pristan
Nayoro
Tumen
Vladivostok
Sapporo
Takikawa
Kraskino
Setana
Khasan
Hakodate
Akita
Ashiro
Baengnyeong Is.
Tono
Hwacheon
Oshu
Yamagata
Sendai
Ganghwa Is.
Chuncheon
Aizuwakamatsu
Nonoichi
Gyeongju
Fukui
Misasa
Busan
Oda
Tsukuba
Yamanashi
Hiroshima
Fujisawa
Yamaguchi
Ishii
Fukuoka
Saga
Kumamoto
Kagoshima
Shuri

B

Gorno-Altaysk
Irkutsk
Okha
Krementui
Manzhouli
Birakan
Tacheng
Manas
Tongliao
Almaty
Aksu
Jiayuguan
Dunhuang
Kashgar
Tianjin
Yinchuan
Laiyang
Lanzhou
Jinan
Leh
Zhenjiang
Chengdu
Wuhan
Lahore
Lhasa
Shanghai
Delhi
Tukuche
Kathmandu
Lijiang
Kunming
Dali
Guangzhou
Vinh Phuc
Taitung
Bhubaneswar
Hanoi
Hyderabad
Yuzhno-Sakhalinsk
Rudnaya Pristan
Nayoro
Kraskino
Sapporo
Takikawa
Setana
Khasan
Hakodate
Ashiro
Baengnyeong Is.
Hwacheon
Oshu
Yamagata
Chuncheon
Nonoichi
Gyeongju
Tsukuba
Busan
Misasa
Oda
Fukuoka
Saga
Kagoshima
Shuri

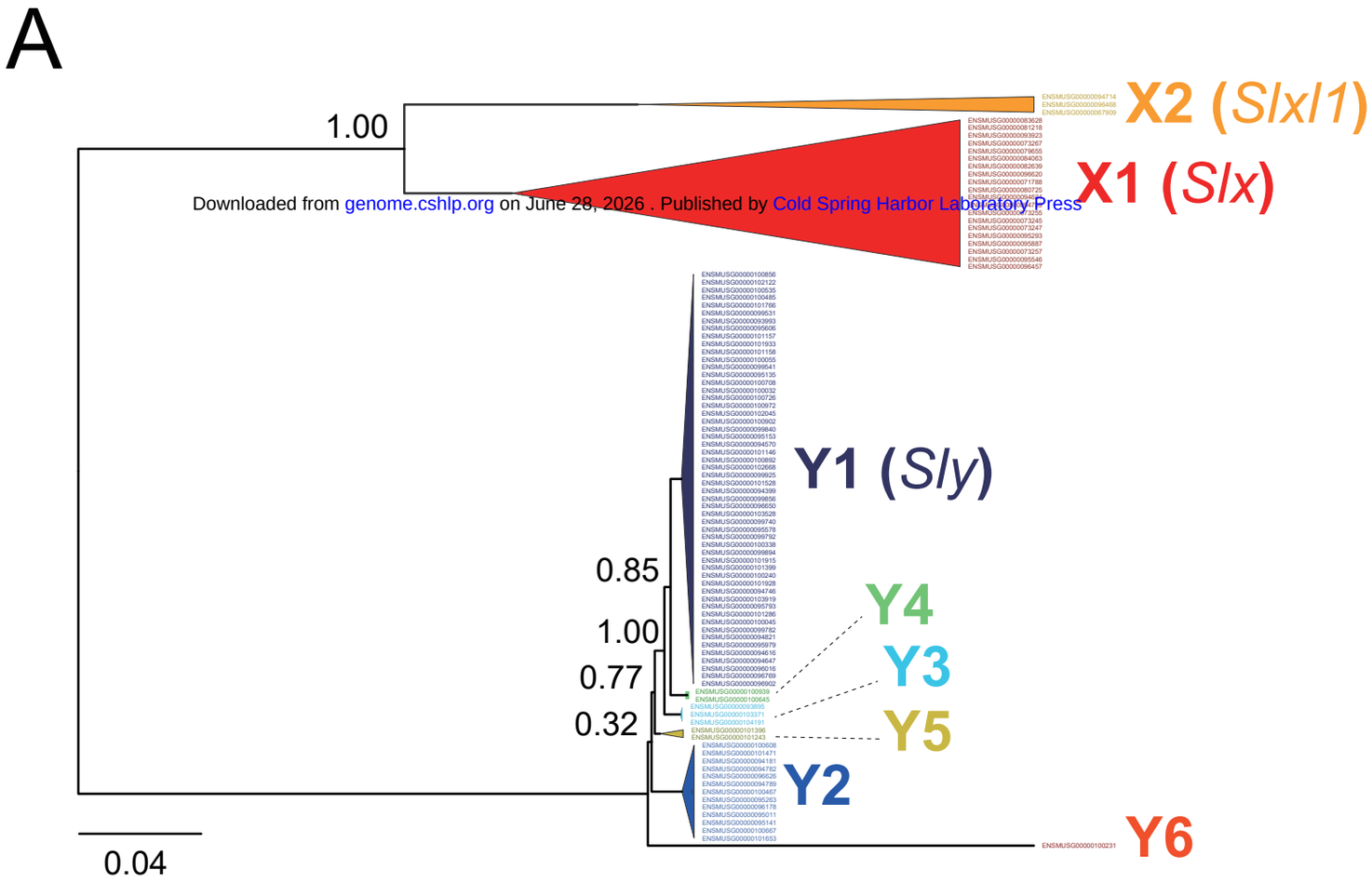

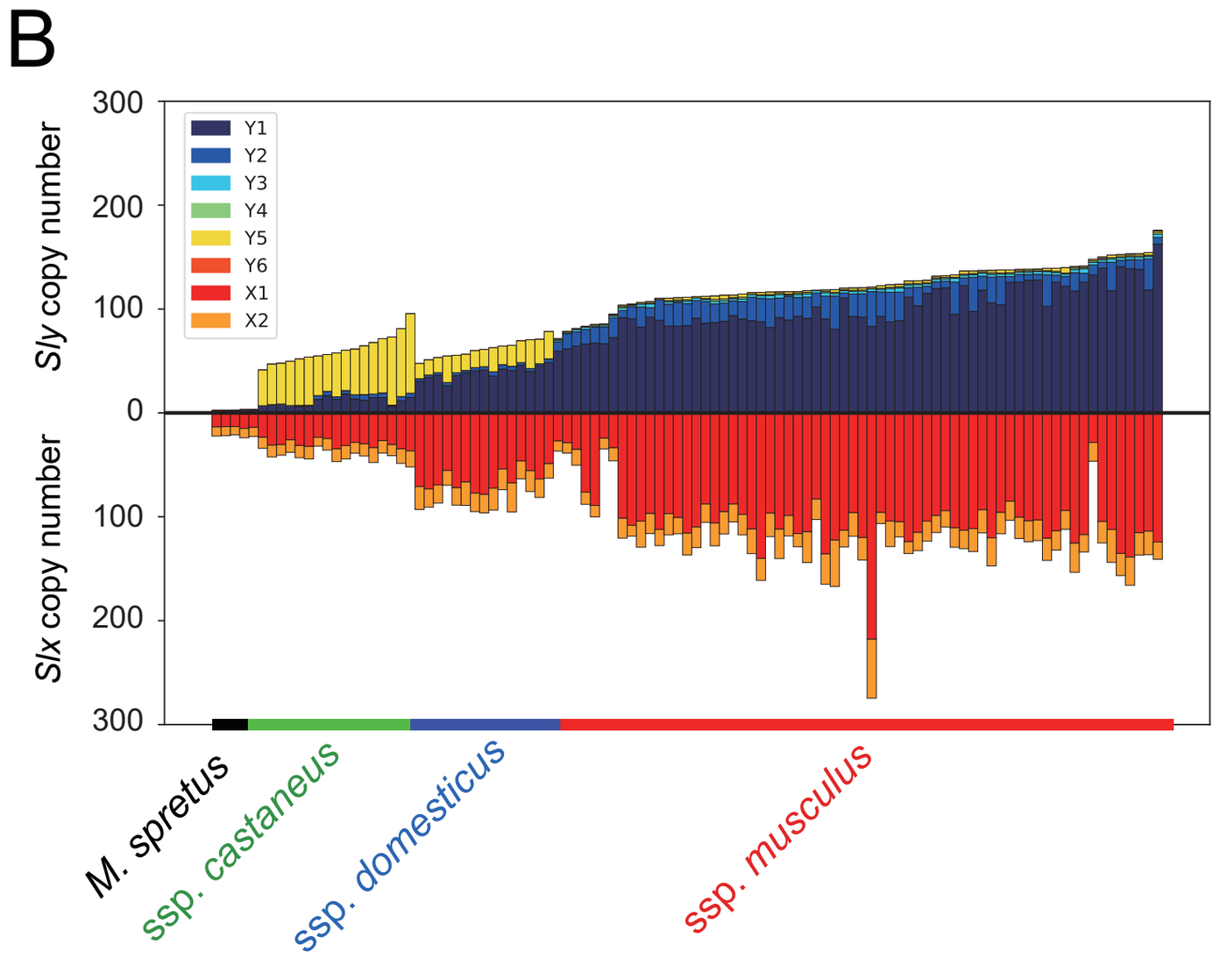

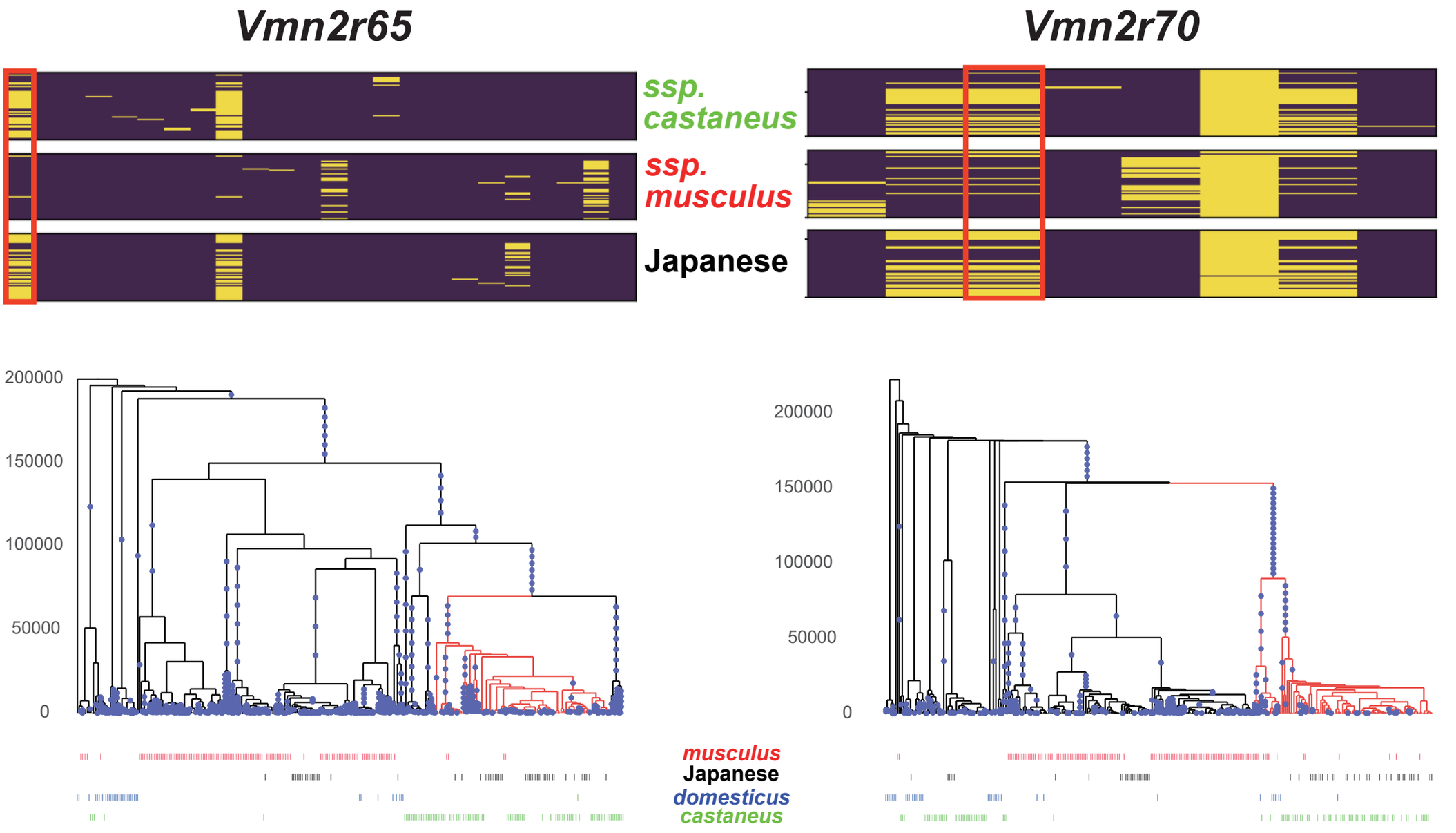
Vmn2r65
Vmn2r70
ssp. castaneus
ssp. musculus
Japanese
200000
150000
100000
50000
0
musculus
Japanese
domesticus
castaneus

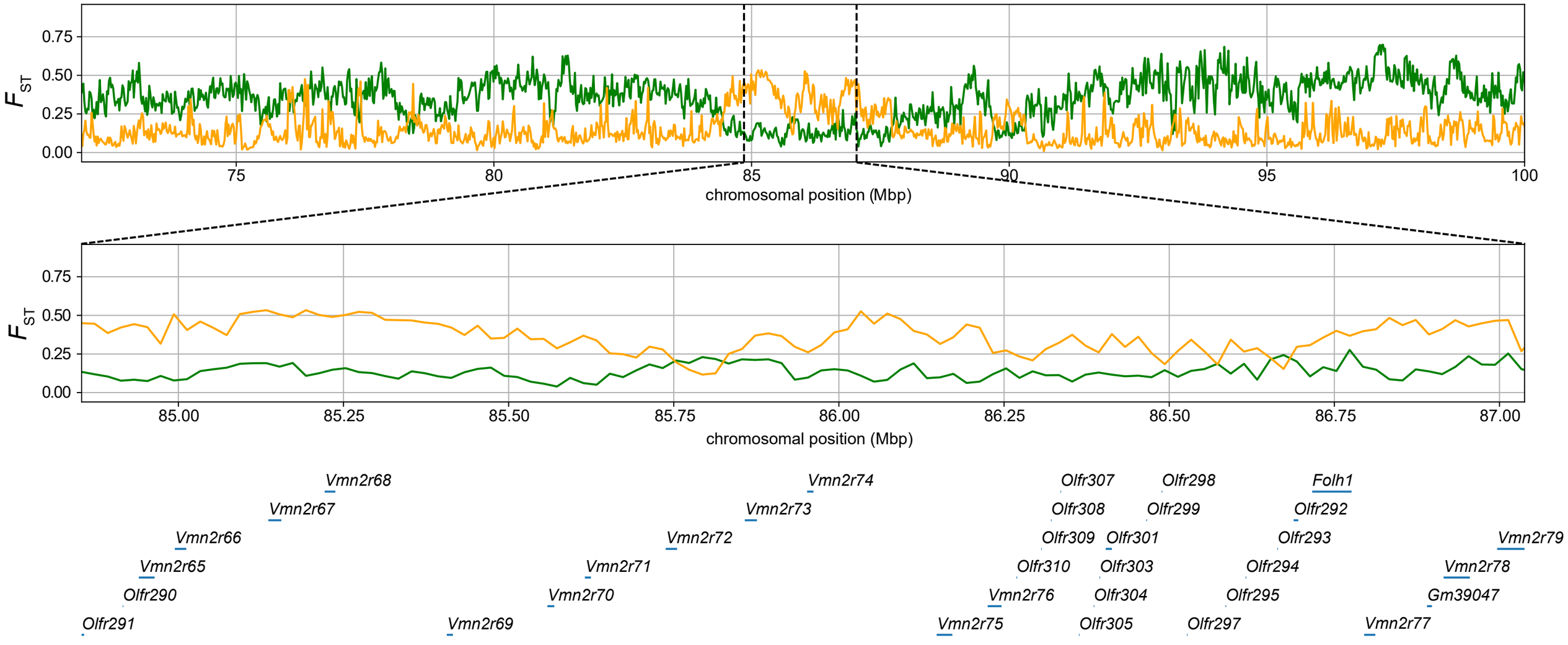
0.75
0.50
0.25
0.00
F_{ST}
75
80
85
90
95
100
chromosomal position (Mbp)
0.75
0.50
0.25
0.00
F_{ST}
85.00
85.25
85.50
85.75
86.00
86.25
86.50
86.75
87.00
chromosomal position (Mbp)
Vmn2r68
Vmn2r67
Vmn2r66
Vmn2r65
Olfr290
Olfr291
Vmn2r69
Vmn2r74
Vmn2r73
Vmn2r72
Vmn2r71
Vmn2r70
Olfr307
Olfr308
Olfr309
Olfr310
Vmn2r76
Vmn2r75
Olfr305
Olfr298
Olfr299
Olfr301
Olfr303
Olfr304
Olfr297
Folh1
Olfr292
Olfr293
Olfr294
Olfr295
Vmn2r77
Vmn2r79
Vmn2r78
Gm39047